Electronic Supplementary Information (ESI) for

Reversible Hydrogen-Bond-Selective Phase Transfer Directed towards Noble Metal Nanoparticles and Its Catalytic Application

Wenjiang Li, Yanhua Wang*, Min Zeng, Jingyang Jiang and Zilin Jin
State Key Laboratory of Fine Chemicals, Dalian University of Technology, Dalian 116024, Liaoning, China
** Corresponding author. Tel.: +86-411-84986033; fax: +86-411-84986033; E-mail address: yhuawang@dlut.edu.cn*

Supplementary Figure

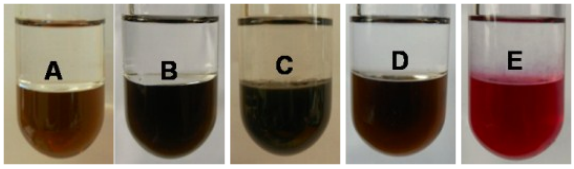

Fig S1. Photographs for the as-prepared NMNPs: (A) Pt-NPs; (B) Ru-NPs; (C) Ir-NPs; (D) Pd-NPs; (E) Au-NPs, in the aqueous (the lower)/1-pentanol (the upper) biphasic system.

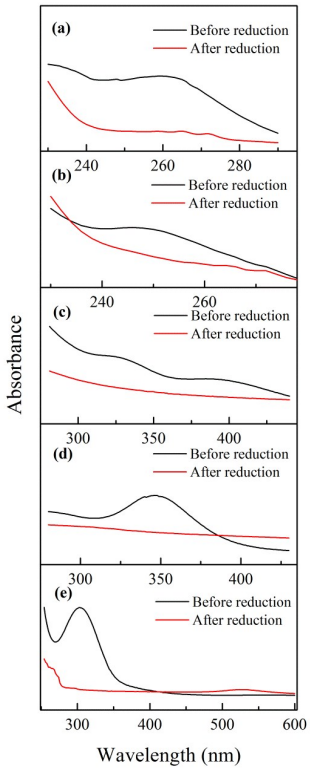

Fig S2. UV-vis absorption spectra of the solutions of thermoregulated ligand/metal precursors (a): $H_2PtCl_6.6H_2O$, (b): $RuCl_3.xH_2O$, (c): $IrCl_3.xH_2O$, (d): $PdNa_2Cl_4.xH_2O$, (e): $HAuCl_4.3H_2O$ in water-ethanol before and after reduction.

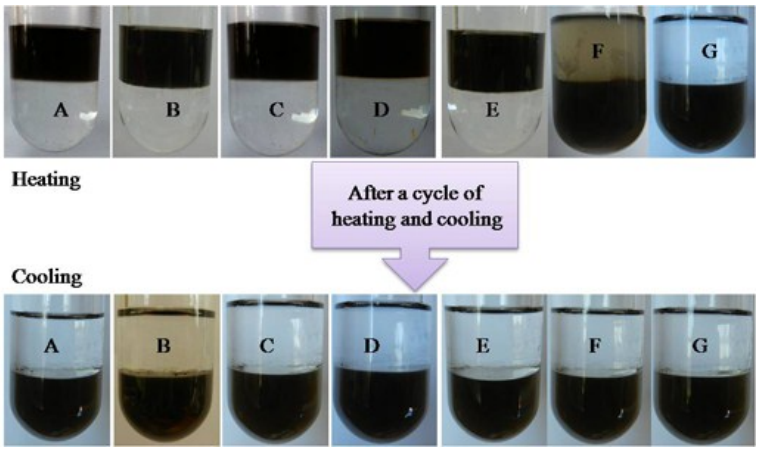

Fig S3. Phase transfer photographs for the as-prepared Ir-NPs between aqueous (the lower) and organic solvents (the upper): (A) 1-butanol; (B) 1-pentanol; (C) 1-hexanol; (D) cyclohexanol; (E) 1-heptanol; (F) toluene; (G) *n*-heptane.

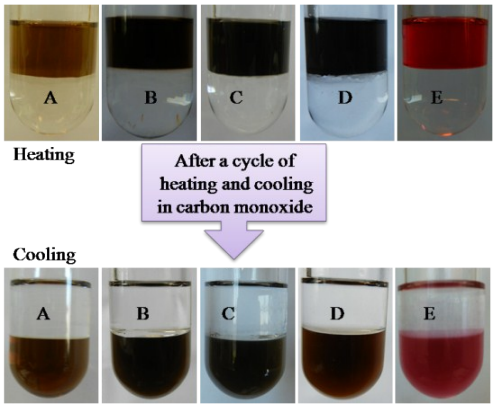

Fig S4. Phase transfer photographs for the as-prepared NMNPs: (A) Pt-NPs; (B) Ru-NPs; (C) Ir-NPs; (D) Pd-NPs; (E) Au-NPs, under carbon monoxide atmosphere in the aqueous (the lower)/1-pentanol (the upper) biphasic system.

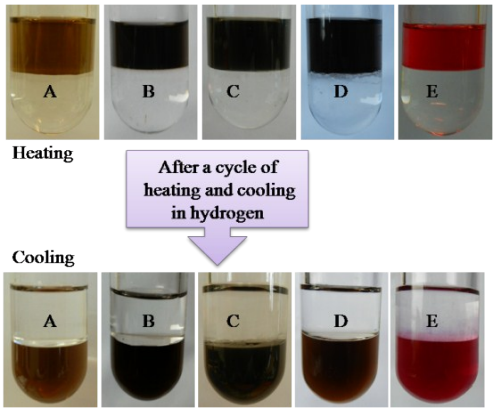

Fig S5. Phase transfer photographs for the as-prepared NMNPs: (A) Pt-NPs; (B) Ru-NPs; (C) Ir-NPs; (D) Pd-NPs; (E) Au-NPs, under hydrogen atmosphere in the aqueous (the lower)/1-pentanol (the upper) biphasic system.

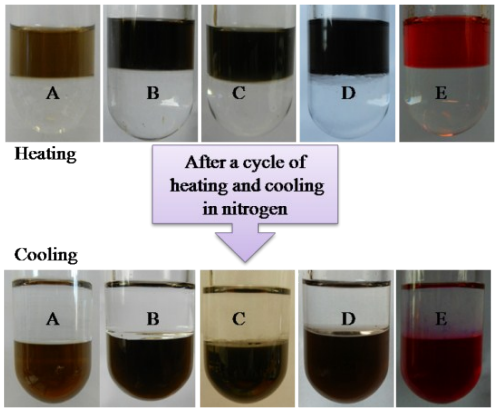

Fig S6. Phase transfer photographs for the as-prepared NMNPs: (A) Pt-NPs; (B) Ru-NPs; (C) Ir-NPs; (D) Pd-NPs; (E) Au-NPs, under nitrogen atmosphere in the aqueous (the lower)/1-pentanol (the upper) biphasic system.

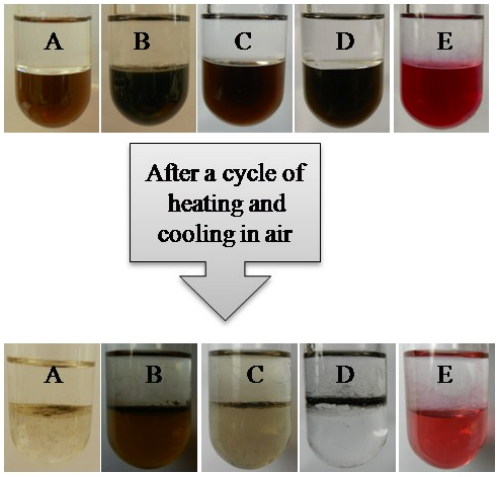

Fig S7. Phase transfer photographs for the as-prepared NMNPs: (A) Pt-NPs; (B) Ru-NPs; (C) Ir-NPs; (D) Pd-NPs; (E) Au-NPs, under air atmosphere in the aqueous (the lower)/1-pentanol (the upper) biphasic system

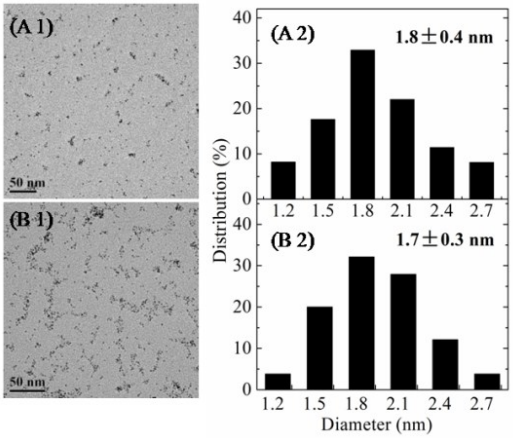

Fig S8. TEM micrographs and particle size histograms of Pt-NPs after one (A1-2) and six (B1-2) cycles of heating and cooling, respectively.

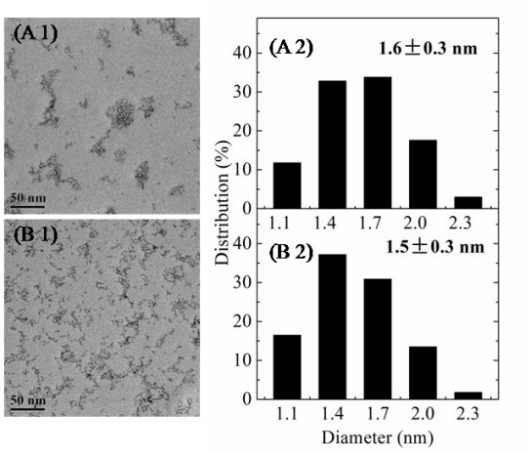

Fig S9. TEM micrographs and particle size histograms of Ru-NPs after one (A1-2) and six (B1-2) cycles of heating and cooling, respectively.

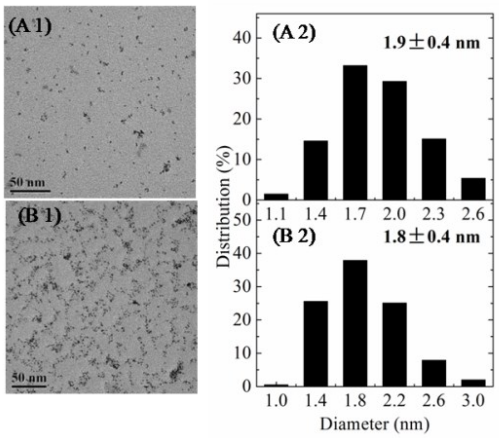

Fig S10. TEM micrographs and particle size histograms of Ir-NPs after one (A1-2) and six (B1-2) cycles of heating and cooling, respectively.

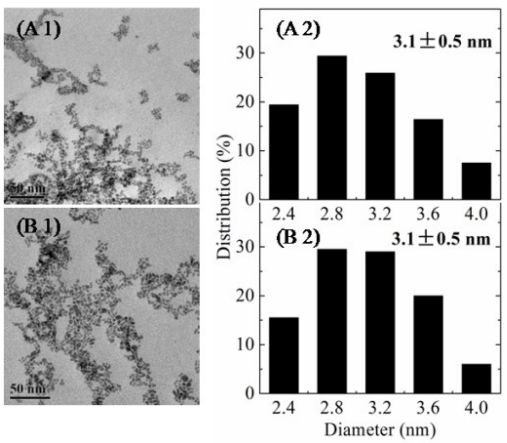

Fig S11. TEM micrographs and particle size histograms of Pd-NPs after one (A1-2) and six (B1-2) cycles of heating and cooling, respectively.

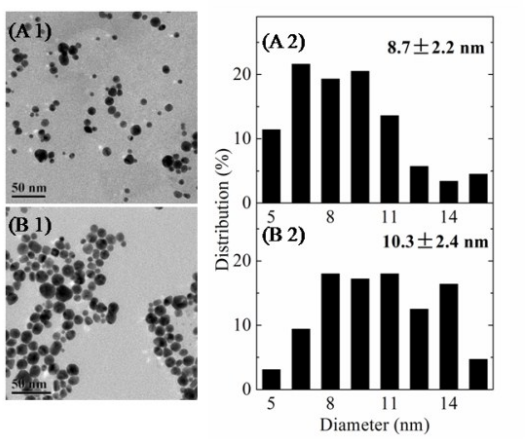

Fig S12. TEM micrographs and particle size histograms of Au-NPs after one (A1-2) and six (B1-2) cycles of heating and cooling, respectively.

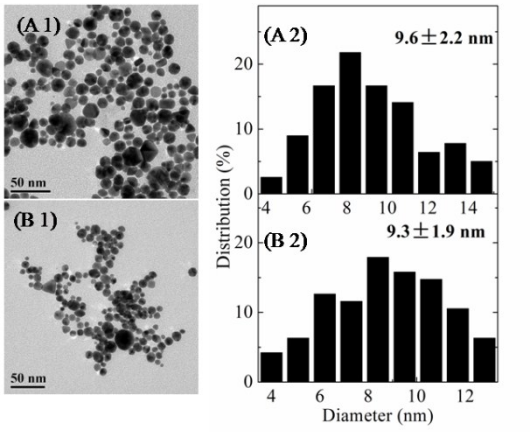

Fig S13. TEM micrographs and particle size histograms about different molar ratios of thermoregulated ligand to Au : 4:1 (A1-2)and 6:1 (B1-2) after six cycles of heating and cooling.

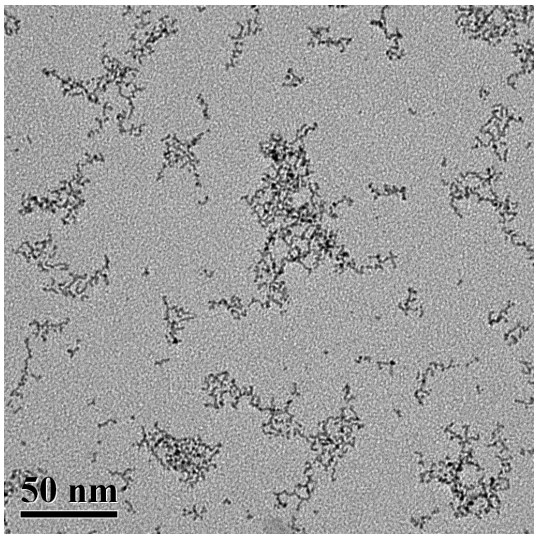

Fig S14. TEM micrographs for Ru-NPs; we can know that the shape of Ru-NPs are not uniform (mainly particulate and linear), leading to agglomeration during the phase transfer process.

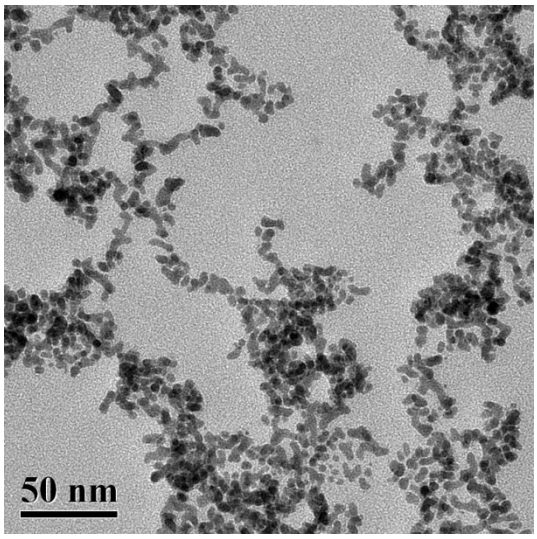

Fig S15. TEM micrographs for Pd-NPs; we can know that the shape of Pd-NPs are also not uniform (mainly particulate and rodlike).

Table S1. The comparative catalytic activity of catalysts for the hydrogenation of DPA around the optimal condition.[a]

Entry	Catalysts	S/C (molar ratio)	Temp (℃)	Time (min)	P (MPa)	DPA conv. (%) [b]	Selectivity (%) [c]	
							Cis-ST	Trans-ST
1	Pt-NPs	500	70	20	1	> 99	86	14
2	Au-NPs	250	70	20	1	-	-	-
3	Ir-NPs	250	70	20	1	6	76	24
4	Ru-NPs	500	70	20	1	7	90	10
5	Pd-NPs	250	70	20	1	30	> 99	-
6	Pd-NPs	250	80	40	1	> 99	> 99	-

[a] Reaction conditions: 1-pentanol 4 mL, water 4 mL, 100 mg of *n*-decane as internal standard. [b] Determined by GC. [c] Diphenylethane (DPE) was not found.

Experimental Details

Synthesis of NMNPs.

For each metal nanoparticles (Pt, Ru, Ir, Pd, and Au), it was difficult to achieve a sufficient dispersion stability and a narrow size distribution in the aqueous/1-pentanol biphasic system (e.g., Ru-NPs and Pd-NPs, Fig S14 and 15) when we just followed the previous method for the synthesis of Rh nanoparticles (see reference 20). So it should be noted that 1) prior to use, one should add distilled water to dissolve each kinds of noble metal salts, completely, with a final concentration as 1 mg/mL; 2) there is a sufficient mixing and dispersing time (about half an hour) before reduction; 3) one should strictly control the reduction time, especially for Au nanoparticles.

Detailed conditions for (1) Ru-NPs were that an aqueous solution of $RuCl_3 \cdot xH_2O$ (1 mL, 3.759×10^{-6} mol), thermoregulated ligand (8.78 mg, 7.518×10^{-6} mol), deionized water (3 mL), 1-pentanol (4 mL) were stirred under hydrogen (4 MPa) at 80 °C for 2 h; (2) Ir-NPs were that an aqueous solution of $IrCl_3.xH_2O$ (2 mL, 6.698×10^{-6} mol), thermoregulated ligand (7.82 mg, 6.698×10^{-6} mol), deionized water (3 mL), 1-pentanol (4 mL) were stirred under hydrogen (4 MPa) at 90 °C for 6 h; (3) Pd-NPs were that an aqueous solution of $PdNa_2Cl_4.xH_2O$ (1 mL, 2.820×10^{-6} mol), thermoregulated ligand (6.70 mg, 5.640×10^{-6} mol), deionized water (3 mL), 1-pentanol (4 mL) were stirred under hydrogen (4 MPa) at 110 °C for 5 h; (4) Au-NPs were that an aqueous solution of $HAuCl_4.3H_2O$ (1 mL, 2.539×10^{-6} mol), thermoregulated ligand (5.94 mg, 5.078×10^{-6} mol), deionized water (3 mL), 1-pentanol (4 mL) were stirred under hydrogen (4 MPa) at 90 °C for 4 h.